Oil & Natural Gas Technology

FWP ESD07-014 - Lawrence Berkeley National Laboratory
FWP 08FE-003 – Los Alamos National Laboratory

Topical Report

Interrelation of Global Climate and the Response of Oceanic Hydrate Accumulations

Submitted by:
Matthew T. Reagan
Lawrence Berkeley National Laboratory
1 Cyclotron Road
Berkeley, CA 94720
e-mail: mtreagan@lbl.gov
Phone number: (510)486-6517

Prepared for:
United States Department of Energy
National Energy Technology Laboratory

Office of Fossil Energy

Interrelation of Global Climate and the Response of Oceanic Hydrate Accumulations

Task Report

Date: June 15, 2013
Period: June 1, 2013 – May 30, 2013
NETL Manager: Skip Pratt

Principal Investigator: Matthew T. Reagan, mtreagan@lbl.gov, (510) 486-6517
Scott M. Elliott, Mathew Maltrud, George Moridis, Philip Jones

Task 3: Testing of the Clathrate Gun Hypothesis

Abstract

It has been postulated that methane from oceanic hydrates may have a significant role in future climate, but the behavior of contemporary oceanic methane hydrate deposits subjected to rapid temperature changes has only recently been investigated. Field investigations have discovered substantial methane gas plumes exiting the seafloor at depths corresponding to the upper limit of a receding gas hydrate stability zone, suggesting the possible warming-driven dissociation of shallow hydrate deposits and raising the question of whether these releases may increase and become more common in the future. Previous work in this project has established that such methane release is strongly regulated by coupled thermo-hydrological-transport processes in the sediments and coupled biogeochemical processes in the water column. In this task report, we discuss the research to date, highlighting the factors that increase or decrease the risk of runaway feedbacks due to climate-driven methane release from the seafloor. The results show that the methane release is likely to be confined to a narrow region of high dissociation susceptibility, defined mainly by depth and temperature, and that any release will be relatively uniform and controlled, rather than explosive. However, coupled ocean simulations indicate that released quantities can be biogeochemically and climatologically significant, as they are similar in magnitude and distribution to the estimated methane release quantities derived from earlier sensitivity studies that suggest significant chemical changes in the water column and significant changes in atmospheric chemistry. This assessment indicates that there are several enhancing and mitigating factors that are still not fully quantified, but even if all positive enhancements are considered, a century-scale injection of methane powerful enough to cause large climate forcing is highly unlikely. However, as warming continues into subsequent centuries, it is likely that much of the methane carbon in shallow hydrates will eventually enter the water column, with significant biochemical and possibly significant long-term climate impacts.

Goal of this report

This report will present both new and previously reported or published results concerning the behavior of hydrates subjected to warming, highlighting contributing and mitigating factors relating to the possibility of rapid climate feedbacks. We will thus assess various scenarios and possibilities for the relationship between climate and hydrates: i.e., the likelihood of a “clathrate gun” event and the mechanisms required for it to occur. The intent is to highlight the most important factors out of the wide range of research results generated by this project. For each section, the referenced papers contain additional information at a higher level of detail.

Models and Methods

The TOUGH+HYDRATE code [Moridis et al., 2008] used in this study describes multiphase flow and transport in hydrate-bearing geologic media. It includes coupled mass and energy transport within porous and fractured media, and also describes the full phase behavior of water, methane, solid hydrate, ice, and inhibitors (i.e. salts). This code was used in previous studies of hydrate dissociation in oceanic sediments [Reagan & Moridis, 2008; Reagan et al., 2011a]. The global ocean simulations are based on a one degree resolution, global Parallel Ocean Program (POP), part of the Community Earth System Model (CESM), a fully-coupled, global climate model that provides state-of-the-art computer simulations of past, present, and future climate states [Gent et al., 2011]. The CESM model is the same described in earlier work in this project [Elliott et al., 2011].

Results

The assessment of the “Clathrate Gun” [Kennett et al., 2000] requires that we integrate four areas of investigation:

1) Ocean warming scenarios, as derived from full Earth system models (ESMs)
2) The processes that occur in hydrate-bearing sub-seafloor systems subjected to warming at the seafloor
3) The processes that occur in the water column, using ocean circulation models (as part of an ESM)
4) The processes that occur in the atmosphere, if hydrate-derived methane is transferred between the oceans and atmosphere

1. Ocean Warming

1.1 Climate Change Scenarios

To assess various climate change scenarios, we use outputs from CESM/POP representing two forward models. One with 4.5 W/m^2 radiative forcing due to CO_2 emissions (RCP4.5), represents a stabilization of CO_2 emissions by 2100 (to approximately 650 ppm equivalent). The second, with 8.5 W/m^2 forcing (RCP8.5), represents a more “business as usual” pathway of increasing emissions through 2100 to over 1,300 ppm CO_2 equivalent with no stabilization [van Vuuren et al., 2001]. To assess temperature changes from preindustrial times to the present, we also use the results of the “Historical” ensemble, which tracks temperature changes from 1855 to 2005/2011 as a “hindcast.” Maps of ΔT vs. location on the 1-degree POP global grid, are shown in Figures 1 through 3.

In Figure 1, we see the hindcast of temperature changes at the seafloor for the period 1855 to the present. For this figure (and subsequent maps), we start first by identifying gridblocks at which the seafloor is within the gas hydrate stability zone (GHSZ) at t = 1855, and at a depth shallower than 1,000 m. This defines a plausible zone of possible hydrate destabilization, as previous work has shown that only hydrates in water depths between 300 m and 1,000 m are likely to be affected by century-scale warming. Then, each subsequent color indicates that a gridblock starting out within the GHSZ has experienced an increase in temperature between 1855 and the present. For the Historical case, it is clear that expected seafloor warming up to the present time is limited, with only 0 ^{o}C - 1^{o}C of warming of existing hydrate-stable zones outside of inland seas or a few small regions around the North Sea, Greenland, Okhotsk, and the Barents Sea.

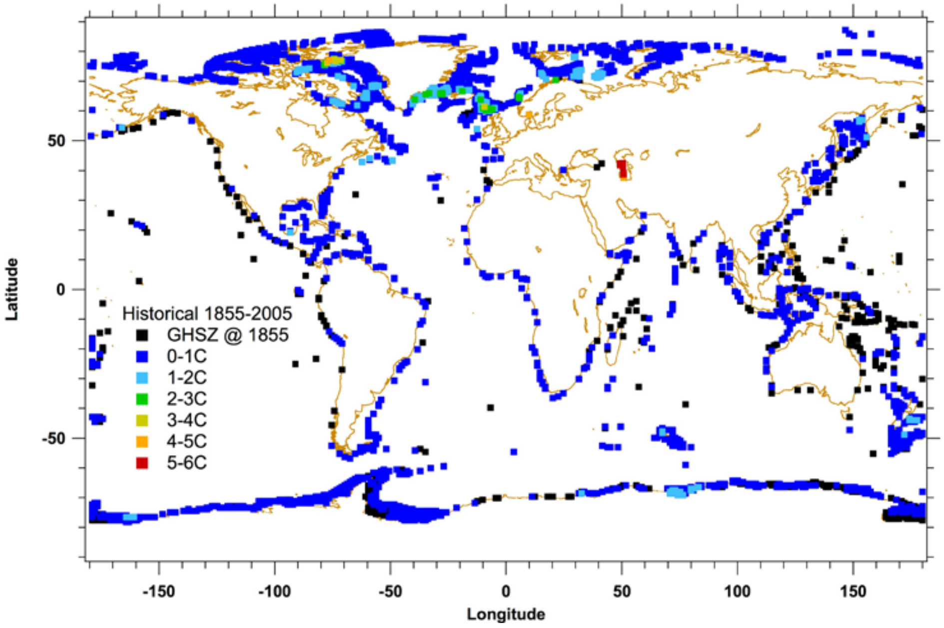

Figure 1: Map of ΔT vs. location on the seafloor for the Historical simulations. Black symbols indicate a GHSZ present at the seafloor at 1855, colored symbols indicate such locations that also experience some positive temperature change.

In Figure 2, we see the first of the forecast models. Here, we map the total temperature increase from 1855 to 2100, following first the Historical ensemble changes, followed by the RCP4.5 forcing scenario. RCP4.5 is best characterized as an optimistic "strong intervention" scenario in which global carbon emissions are strong curtailed. It is thus a good lower-bound for hydrate destabilization estimates.

For RCP4.5, we see that warming of 1 ^{o}C - 2^{o}C is widespread across historically hydrate-stable, sensitive regions of the Arctic basin seafloor by 2100, with notable warming in the North Sea, Barents Sea, near Greenland, and in Okhotsk. Also notable is seafloor warming off the South Carolina coast (perhaps upslope from Blake Ridge), the New Zealand margin, the Gulf of Mexico, and some parts of the Antarctic coast. Only a few gridblocks, however, fall into the +3^{o}C - +5^{o}C range that previous simulation studies have suggested as a driver for strong hydrate dissociation and methane gas release [Reagan et al., 2011b].

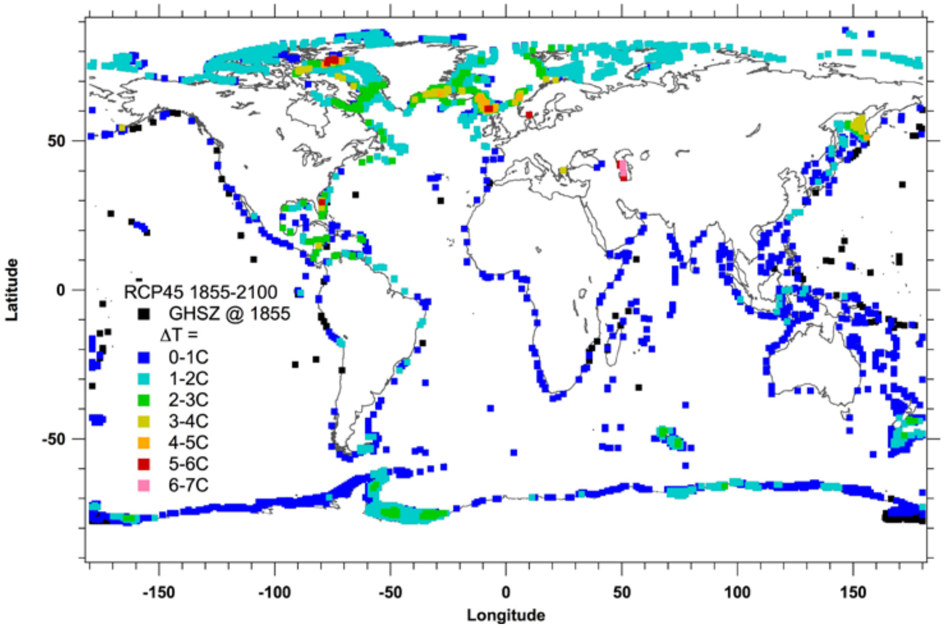

Figure 2: Map of ΔT vs. location on the seafloor for the RCP4.5 simulation. Black symbols indicate a GHSZ present at the seafloor at 1855, colored symbols indicate such locations that also experience some positive temperature change.

Figure 3 maps temperature changes for the strongest warming scenario, RCP8.5. Recent observations comparing warming to-date with various forecasted scenarios suggest that, barring rapid political shifts and dramatic reductions in emissions, this scenario is becoming more and more likely to represent the pathway for the coming century.

For RCP8.5, significant warming (+3^{o}C or more, as defined by previous simulation studies) is widespread across sensitive regions of the Arctic basin margin, with the strongest warming in the Barents Sea, North Sea, Greenland margin, United States East Coast, New Zealand margin, and Okhotsk. Temperature increases of +4^{o}C - +5^{o}C have become more widespread. Moderate to significant warming has also spread to the Beaufort Sea, the edge of the East Siberian Arctic Shelf, and the expanded along the Antarctic Peninsula.

For this relatively “warm” scenario, it is important to note that the bulk of the sensitive hydrates subjected to significant warming within the next century are largely grouped along the margins of the Arctic Basin. This is consistent with assumptions made in previous simulation studies [Elliott et al., 2011;Reagan et al., 2011b].

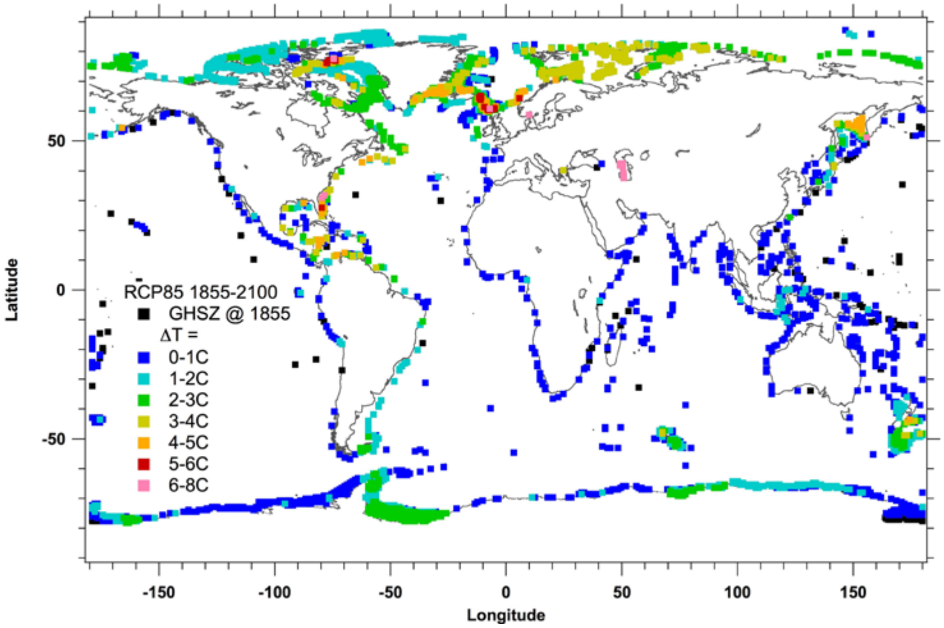

Figure 3: Map of ΔT vs. location on the seafloor for the RCP8.5 simulation. Black symbols indicate a GHSZ present at the seafloor at 1855, colored symbols indicate such locations that also experience some positive temperature change.

1.2 Hydrate Destabilization

While warming is widespread for the most strongly forced scenario (and not to be ignored for the moderate scenario), only temperature changes affecting hydrates already near the edge of the GHSZ can cause dissociation and methane release. Figures 4 and 5 show where near-term dissociation could be possible.

In Figure 4, we generate another map of the historical GHSZ at $t = 1855$, and then overlay gridblocks in which the warming shown in Figure 1 moves the seafloor out of the GHSZ by the present day, according to the TOUGH+HYDRATE physical properties routines [Moridis et al., 2008]. Regions of potential hydrate existence and present-day destabilization are limited, with only a few areas within the Barents Sea and the North Atlantic margin containing more than a few gridblocks subjected to sufficient warming. Also overlayed on the map are gridblocks with +3^{o}C warming, or greater, and such locations are very limited. While this POP/CESM grid is quite coarse, it is clear that while localized warming could be manifesting itself in the present day, such warming is not yet widespread in shallow, sensitive, hydrate-bearing regions and visible at a global scale. Warming-driven methane releases are thus likely to be very limited and localized at this date.

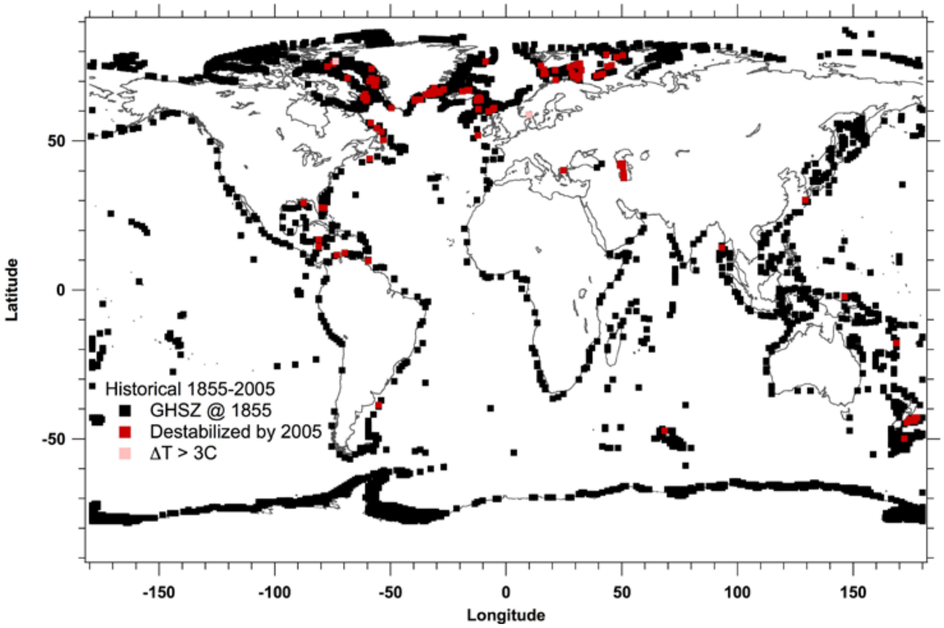

Figure 4: Map of potential regions of hydrate destabilization for the Historical scenario. Black symbols indicate a GHSZ present at the seafloor at 1855, red symbols indicate such locations that have been moved outside the GHSZ by seafloor warming.

In Figure 5, we plot the same map for the RCP8.5 scenario. The warming in this scenario drives a large region of the Arctic Basin out of the GHSZ by 2100, with warming of over +3^{o}C widespread throughout the Barents Sea, Greenland margin, North Sea, and in a thin zone along the North American East Coast. Also notable is the lack of destablization along the Antarctic coast, where the data shows significant seafloor warming.

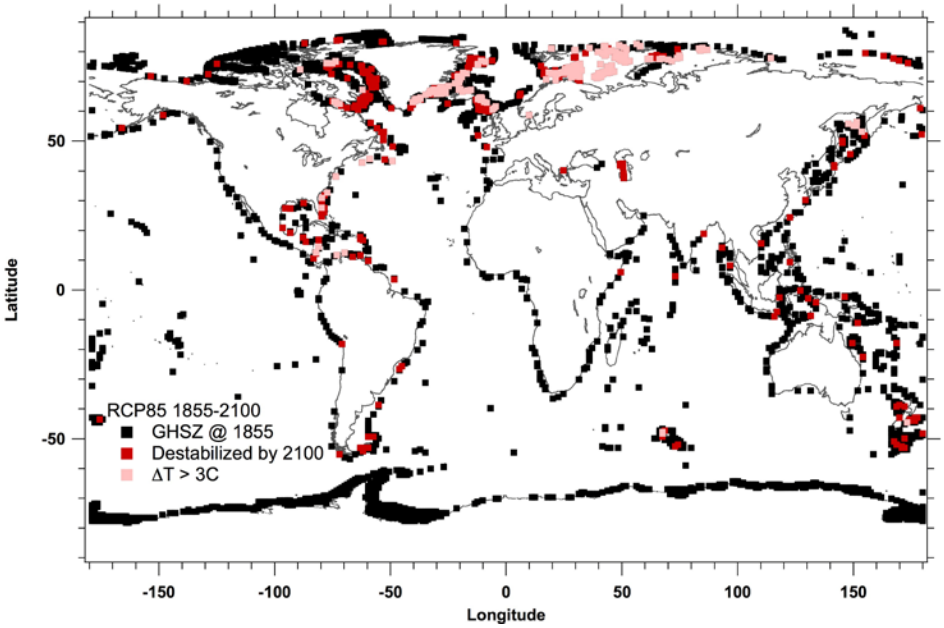

Figure 5: Map of potential regions of hydrate destabilization for the RCP8.5 scenario. Black symbols indicate a GHSZ present at the seafloor at 1855, red symbols indicate such locations that have been moved outside the GHSZ by seafloor warming, pink symbols indicate destabilized locations with warming of +3^{o}C or more.

In Figure 6, we replot the data on a polar plot centered on the North Pole to zoom in on the critical regions for hydrate destabilization. Without the distortion of a Mercator-style project of the grid, it is easy to see the strong warming and destabilization of the preexisting GHSZ throughout the Barents Sea, along the Greenland margin, and at a few locations within Okhotsk.

The critical take-away from this analysis is that even for climate scenarios with strong forcings (not necessarily a “worst-case” scenario but one on the upper end of likely outcomes), destabilization of hydrate on the century scale is limited and localized. While hydrates are ubiquitous in the oceans, only a subset of those hydrates are sensitive to short-term climate changes in such a way to create large methane releases, fast feedbacks, or tipping points.

However, this still leaves a large reservoir of sensitive hydrates. The total area of the POP/CESM gridblocks shown in Figure 5 is approximately 1.28M square kilometers (areas of seafloor within the GHSZ), and the area of the pink gridblocks (+3^{o}C or greater) is 475,000 square kilometers of seafloor. Additional warming over longer timescales is likely to push more and more of the seafloor into destabilization, although as depth increases, the required change in temperature will become larger, mitigating the process.

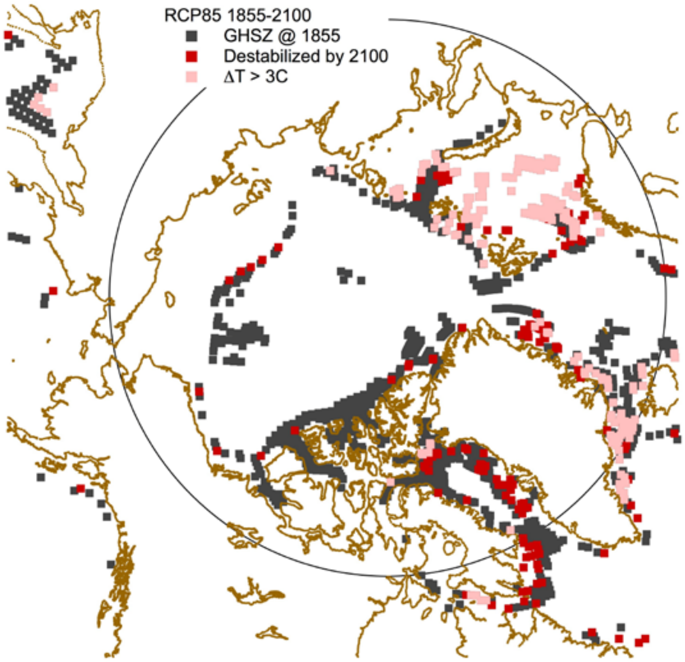

Figure 6: Polar map of potential regions of hydrate destabilization for the RCP8.5 scenario. Black symbols indicate a GHSZ present at the seafloor at 1855, red symbols indicate such locations that have been moved outside the GHSZ by seafloor warming, pink symbols indicate destabilized locations with warming of +3^{o}C or more.

2. Sub-seafloor processes

2.1 Temperature change and depth effects on hydrate dissociation

Hydrates near the edge of the GHSZ, as described in the previous section and in early work in this study [Reagan et al., 2008], can be destabilized by small temperature changes, and release significant methane into the sediments and possibly into the water column. However, more substantial temperature changes, acting on shallow hydrate deposits near the stability limit, are required to generate larger gas-phase fluxes of methane [Reagan and Moridis, 2008; Reagan et al., 2011b]. Even small changes that generate smaller yearly fluxes (primarily aqueous phase) will continue to drive hydrate dissociation and methane release for centuries, until a new equilibrium is reached [Reagan and Moridis, 2008; Reagan et al., 2011a;b].

At this point, our study has only addressed century-scale events, with temperature changes of +1^{o}C, +3^{o}C, and +5^{o}C over 100 yr applied to the top of the hydrate system, followed by several centuries of constant temperature. This allows the system to reequilibrate over time, forming a new geothermal gradient and a new configuration of hydrate and gas within the sediments. In published work, system evolution has typically been tracked for 100 - 300 yr, with temperature changes imposed at the seafloor for only the first 100 yr (as values for temperature changes beyond 100 yr are increasingly uncertain). In every case, methane release at the seafloor continues after the first century with only a moderate fall-off in the rate of methane transport [Reagan et al., 2011a;b]. In many of these cases (in all cases of shallow hydrates) the hydrate eventually dissociates completely after 200-300 yr with transport of methane via gaseous and aqueous phases continuing for some time afterward.

Figure 7, from Reagan et al. [2011b], presents cumulative methane release curves for two schematic warming scenarios. The left panel is for a system where the degree of warming decreases with depth, from +5^{o}C at 350 m depth to +1^{o}C below 550 m depth (simulations performed prior to the CESM/POP assessments of global ocean temperature change shown in Section 1). In the right panel, hydrates at all depths were subjected to a +5^{o}C temperature increase at the seafloor (as indicated by the maps in Section 1, this represents an extreme warming event). For all scenarios, warming proceeds for 100 yr, after which temperature at the seafloor is held constant. Note the log scale in *y*. The shallowest hydrates contribute nearly all of the released methane for both scenarios, with orders-of-magnitude decreases in total methane release below 450 m depth. This indicates, in parallel with the equilibrium assessments of stability derived from climate models in Section 1, that only a narrow "bathtub ring" of sensitive and readily dissociating hydrates can contribute to short-term methane releases.

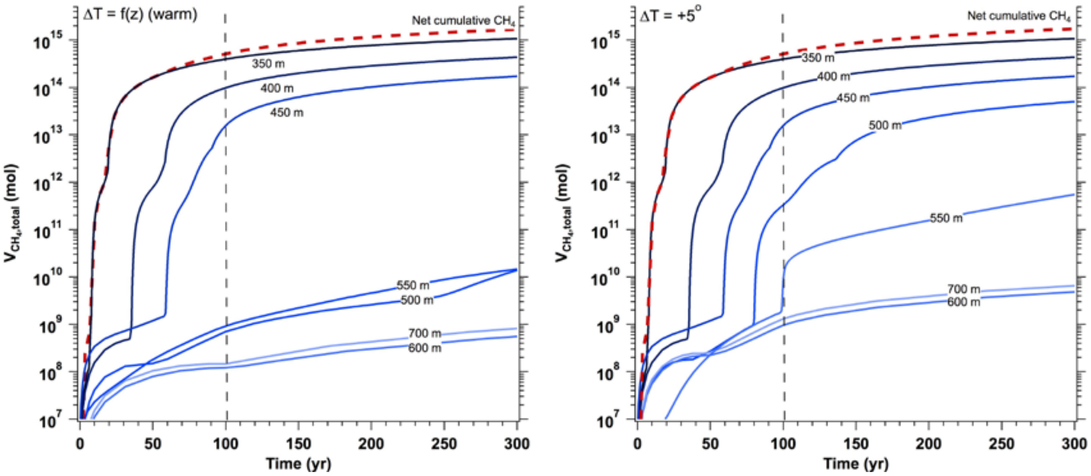

Figure 6: Cumulative methane release into the water column vs. time for two Arctic warming scenarios from Reagan et al. [2011b], including total release over the Arctic basin (red line) and binned by depth intervals.

If temperature change continues, rates of dissociation could increase in future centuries, but the constraint mentioned earlier still applies—shallow hydrates near the edge of the GHSZ, while most likely to dissociate, are also by definition thinner deposits, and as such contain enough hydrate to release methane for only a few hundred years before exhaustion [Reagan and Moridis, 2008; Reagan et al., 2011b]. Delays in the transport of methane between the dissociation front (which is moving deeper into the sediment column over time), along with the self-limiting nature of the dissociation due to heat-transfer limitations [Reagan and Moridis, 2008], ensure that methane release will not increase exponentially over time even with additional warming, but rather remain an "orderly" process leading to roughly flat release vs. time curves.

Most studies (notably Biastoch et al., 2011 and Hunter et al., 2013) use a stand-alone heat diffusion model to track the propagation of temperature changes into the sediments, and assess hydrate dissociation by comparing the change in temperature to an equilibrium hydrate formation model, discounting the coupled flow-thermodynamic-transport effects that occur during dissociation. They therefore conflate (unintentionally perhaps) hydrate *dissociation* with methane *release*. Taking the cumulative release curves from Reagan et al. [2011b] and dividing by the cumulative quantity of methane released into the sediments through hydrate dissociation, we can track the percentage of hydrate-derived methane (release ratio) that actually reaches the seafloor vs. time.

Figure 8 shows the release ratio for two of the simplified warming scenarios from Reagan et al. [2011b]. As in Figure 7, the left panel is for a system where the degree of warming decreases with depth, from +5^{o}C at 350 m depth to +1^{o}C below 550 m depth. Release ratio is plotted over 300 yr, with warming occurring in the first 100 yr, followed by 200 yr of constant temperature at the seafloor. In the right panel, hydrates at all depths were subjected to a +5^{o}C temperature increase at the seafloor, an extreme event. For both scenarios, we see that the majority of the methane in the sediments does not reach the seafloor within a multi-century timescale. The shallowest, most sensitive, and most productive systems at 350 m water depth transport only 13% of the hydrate-derived methane into the water column within the first century, with the release ratio leveling at approximately 15% as two more centuries pass. Hydrates at depths below 500 m send only a small fraction of their methane into the water column on these time scales. The dotted curves provide the total release ratio for hydrates at all depths, integrated over the Arctic basin and weighted by seafloor area [Reagan et al., 2011b]. The total release ratio levels off at or below 13% for either scenario. It is important to note that these ratios are calculated for relatively permeable sediments, with low irreducible gas saturation, and it is simple to model alternative systems capable of retaining an even greater percentage of gas.

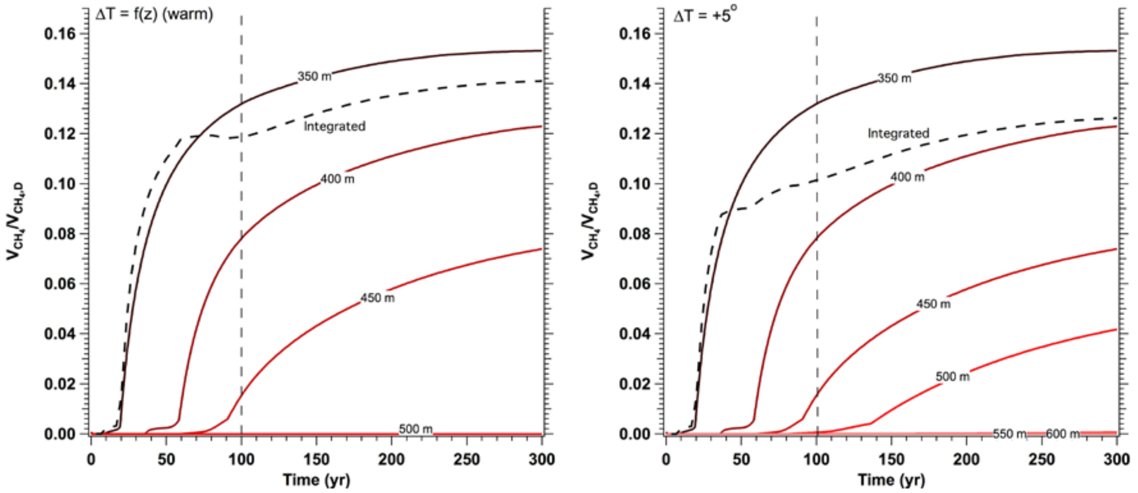

Figure 8: Release ratio (cumulative methane release at seafloor / cumulative hydrate dissociation) for two warming scenarios, for several depth intervals and the total integrated set of release curves. Release curves from Reagan et al. [2011b].

Other depth- and temperature-related effects have been studied by various TOUGH+HYDRATE simulation studies, including within this project [Reagan and Moridis, 2008] and others [Thatcher et al. 2013]. Relevant discoveries include:

- Only large increases in ocean depth, possibly occurring *before* warming commences, can significantly mitigate the sensitivity of shallow hydrates to ocean warming [Reagan and Moridis, 2008]
- While the magnitude of warming directly drives the magnitude of methane release [Reagan and Moridis, 2008; Reagan et al., 2011a;b], the difference between rapid/step changes in temperature and linear changes on the century scale, for the same ΔT, is not great, due to the heat transfer limitation discussed in Section 2.2
- Hydrate systems in deeper water, with initial temperatures that place them further from the edge of the GHSZ, are unlikely to be sources of gaseous methane, as 1) temperature changes must propagate deeper into the system before dissociation begins, 2) dissociation may begin from the bottom of the deposit, and 3) the overlying zone of hydrate stability would hinder the transport of methane to the seafloor [Thatcher et al. 2013; Reagan and Moridis, 2008].

Not addressed in this project is the reaction of ocean hydrates to long-term, sustained climate change, perhaps time periods far longer than the rapid changes postulated in the Clathrate Gun hypothesis. Clearly, heat-transfer and transport limitations place strong limits on the release of hydrate-derived methane, even if one assumes that the actual hydrate reservoir is large and that hydrates exist at all location where a GHSZ has been present. However, when and if warming continues over several centuries, hydrates at deeper locations will necessarily fall into the "sensitive" category, with the pressure-dependence of the phase diagram mitigating the process below approximately 1000 m [Reagan and Moridis, 2008] (i.e., for deeper hydrates, temperature changes would have to be progressively larger with depth, eventually exceeding the larger predicted changes). While these releases would be constrained in the same fashion as those from shallow deposits—i.e. subject to the same heat-transfer limitations—it would extend the period of "chronic" release of methane for centuries. Simulation studies of long-term warming are necessarily to assess this scenario.

2.2 Sediment properties and hydrate dissociation

Sensitivity studies were a key component of this study, particularly during the early assessments of hydrate stability and the discovery of the processes that govern climate-driven hydrate dissociation [Reagan and Moridis, 2008; Reagan et al. 2011a;b] and exploration of the simulation parametric space has continued with a focus on recently explored natural systems [Thatcher et al. 2013]. The key discoveries in this area are:

- All but the lowest-permeability sediments result in some methane release, and continuous methane release over century timescales [Reagan and Moridis, 2008; Reagan et al., 2011a], however,
- Very low-*k* sediments enhance hydrate self-preservation effects through localized increases in pressure [Reagan and Moridis, 2008; Thatcher et al. 2013], and methane transport may be limited to cases where overpressure fractures the sediments near the seafloor [Thatcher et al. 2013]
- The rate-limiting step for hydrate dissociation is heat-transfer limitations, coupled with the endothermic nature of hydrate dissociation [Reagan and Moridis, 2008; Reagan et al. 2011a], however,
- Variations in heat flow, initial hydrate saturation, and sediment thermal properties affect the rate of dissociation, but not drastically [Reagan et al. 2011a; Thatcher et al. 2013], as long as the deposits are near the edge of the GHSZ.

We expect that shallow hydrate systems, in reality, lie in heterogeneous geological environments [Thatcher et al., 2013] such that the 1-D or homogeneous 2-D hydrate models used to assess dissociation and methane transport are likely to under-predict the localized methane release while providing a reasonable estimate of widespread dissociation potential. This is due to expected methane movements along lower-*k* pathways, including faults, channels, horizontal motion between strata of varying permeability, and localized release through chimney, vents, or other heterogeneities at the seafloor itself. For example, the plumes observed off Spitsbergen can be explained both by local channeling of methane by both the heterogeneous sedimentary system and interference by a preexisting GHSZ [Thatcher et al., 2013], while the total estimated release is close to that made by simulating homogeneous dissociation in 1D or 2D [Reagan et al, 2011a]. As such, one expects that models can suggest the coarse regional distribution of methane release and the total potential flux, while the nature of the actual release into the water column (disperse aqueous flux/bubbles vs. focused plumes with high flow rates) will be a function of the (typically unknown and unmapped) local geology and topography.

2.3. Attenuation by anaerobic oxidation of methane (AOM) at the seafloor

Preliminary simulation of methane consumption (and therefore injection as CO_2 rather than CH_4) through AOM processes at the sediment-ocean interface suggest that low-flux release scenarios, particularly via aqueous transport only, are likely to be at least partially attenuated. Although such CO_2 injections may have local biochemical consequences (see Section 3), compared to anthropogenic emissions. For example, the releases shown in Section 2, Figure 6, give an average release of 6.6 Tmol of CH_4, which if fully oxidized, would give 300M metric tones of CO_2, much smaller than the 9,200M metric tons of CO_2 released yearly from manmade sources.

If hydrate-derived methane is to serve as a strong feedback, release of methane into the water column, and eventually the atmosphere, is necessary. Only higher-flux scenarios, perhaps through a combination of gas-phase transport and enhancing by focusing of plumes through local heterogeneity, are likely to push much of the methane past the thin AOM zone into the water column [Reagan et al., 2008]. We therefore have focused on determining the mechanisms and likelihood of these strong-release scenarios, rather than incorporating more detailed treatment of AOM in the coupled model.

3. Water column processes

3.1 Resource limitations to methane oxidation

In previous work, methane fluxes from the initial sediment-column simulations were forward-coupled into the offline POP/CESM ocean model, with the addition of water column methane biochemistry. The results demonstrated that the hydrate-driven methane releases are sufficient to cause both significant acidification near the source, plus localized hypoxia in poorly ventilated basins subjected to even the baseline level of methane fluxes [Elliott et al., 2011]. Furthermore, biogeochemical analysis revealed that regional scale depletion of the key nutrients nitrogen, iron and copper may ensue [Elliott et al., 2010]. If any single resource is lacking the methane plumes could stabilize, and approach to the atmosphere becomes possible.

Figure 9 shows methane concentration in the water column for a simulation with a full methane cycle at t = 30 yr. Note that releases along the Arctic shelf result in only localized spikes in concentration, while poorly ventilated basins like the Bering Sea or Okhotsk accumulate much more methane.

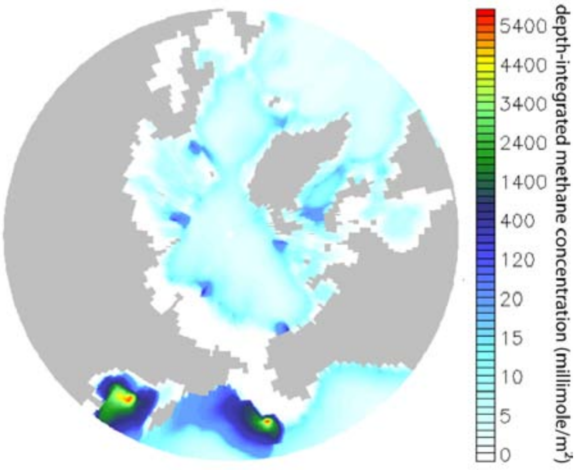

Figure 9: Methane concentration in the water column at t = 30 yr for a system with oxygen limitation.

Figure 10 shows the biogeochemical consequences of such methane release. The left panel plots oxygen concentration in the water column at t = 30 yr. Note the virtual hypoxia created by the oxidation of methane in the poorly ventilated Bering Sea and Sea of Okhotsk. In such a case, methane consumption would be limited by lack of available oxygen, increasing the probability of transfer to the atmosphere. The right panel plots water column pH, showing the ocean acidification caused by the generation of CO_2 during methane oxidation. Again, changes are localized near plume locations, but the effects spread across the Arctic basin (a slight effect) and with stronger effects throughout the Bering Sea and Okhotsk. These results are particularly important in that they highlight an unforeseen biochemical consequence of hydrate dissociation.

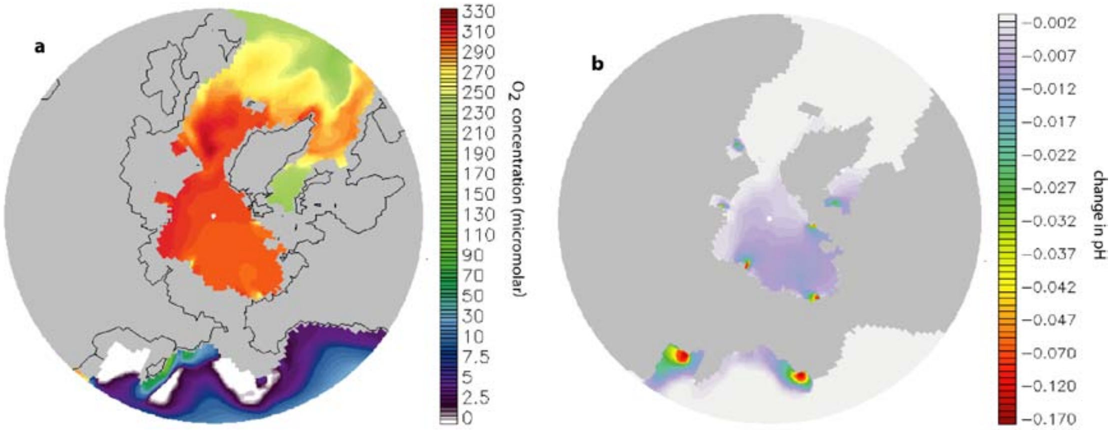

Figure 10: Oxygen concentration (left) and pH (right) at *t* = 30 yr for ocean systems subjected to methane release.

The initial ocean transport simulations revealed unexpected geographic (fluid dynamic) channels for transport toward the surface mixed layer, even when the methane is fully dissolved. Plumes of CH_4 do not simply follow the Atlantic Layer in its circuit of the polar shelf break. Upward mixing along the slope and by other mechanisms leads to up to 10% transfer of methane into the atmosphere even when the methane cycle and methane oxidation is included. At the upper limit, if resource limitations shut down methane consumption, much larger transfers to the atmosphere are possible even without transport by gas plumes. Figure 11 shows the ratio of hydrate-derived methane released to the atmosphere in the model for fully non-reactive methane, representing the most extreme case of resource limitation. About 60% of the methane is able to reach the mixed layer and the atmosphere even though no plume transport has occurred and the methane was fully dissolved at depth. This 10%-60% range of release is expected to increase as bubble plume processes are included in the model and methane is permitted to dissolve at shallower depths, or even reach the surface in the gas phase.

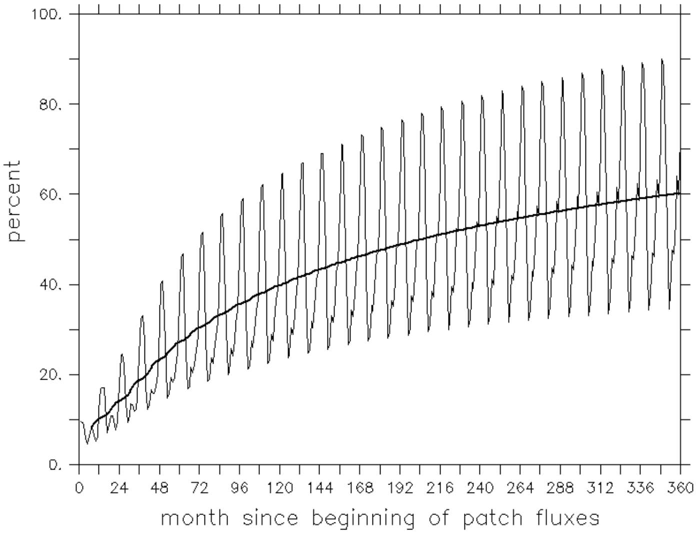

Figure 11: Methane transfer to the atmosphere for nonreactive methane.

3.2 Bubble-plume transport

The ocean simulations in Section 3.1 assumed full dissolution, i.e. addition of methane at 300 m depth in the aqueous phase only. In reality, the hydrate dissociation and subseafloor transport simulations indicate that for large fluxes of methane to occur, transport must be primarily in the gas phase [Section 2; Reagan et al., 2011b]. Comparison of 2D hydrate dissociation simulations with estimated gas-plume extent seen off the Spitsbergen margin [Westbrook et al., 2009] suggest that that fluxes indicated in the simplified simulation cases are approximately of the same magnitude as the observed plumes [Reagan et al., 2011a], suggesting that the physical manifestation of the predicted methane releases will be primarily in the gas phase, and that such releases can feed substantial gas plumes, particularly if gas release over a wide area is channeled through a limited set of fractures or other heterogeneities on the seafloor [Thatcher et al., 2013].

Therefore, a bubble-plume parameterization has been added to POP/CESM to capture the mechanisms that control the delivery of dissolved methane to the water column (i.e., at what depth does the dissolution occur, and what percentage dissolves before escape to the atmosphere). Approximations were introduced such that vertical exponential decay applies to gas phase concentrations at a depth of 500 m or less. Observations of actual cold water bubble behavior served as a starting point for the parameterization [Rehder et al. 2002; Leifer and MacDonald, 2003]. Bubbles may accumulate organic surfactant coatings that will render their surfaces rigid, leading to a slight depression of the buoyant rise rate. But more importantly, film formation will thicken the laminar layer barrier to methane dissolution back into the water column. Bubble sizes are bracketed at the low end by creep flow, which is assumed to enforce local injection, and on the high side by oscillatory breakdown [Leifer and Patro, 2002]. An advective-removal steady state form is used to estimate the fate of a typical rising bubble field. Considerations of gas nonideality are combined at elevated oceanographic pressures with buoyancy-drag, geometric dynamics, and surfactant effects. Numerical integrations upward from the sea floor show that pressure release and expansion compensate mass loss for bubbles approaching 1 cm, with the maximum dictated by turbulent subdivision in the column. Below 1 cm diameter, dissolution is shown to occur well within a circulation model grid layer.

To initialize the vertical redistribution process, concentration is set just above the sediment interface by flux matching against the methane gas output. A single equation then determines gas dissolution rates by apportioning total input over the entire water column. An additional fraction may be released through the sea surface to the atmosphere. This release is most significant for bubble with radii approaching 1 cm. Uncertainties explored in our calculations include the potential for an early boost phase attributable to inert giant bubbles, bulk fluid interactions leading to vertical acceleration of the water column itself [Leifer et al. 2009], and the option for clean surfaces to dominate in remote areas [Rehder et al. 2002].

As a means of validation for this approach, we compare gas phase concentration fall off, solute buildup and plume tilt estimates with data available for several known Arctic methane sources [Westbrook et al. 2009]. For the base line case involving 3 mm bubbles coated with a generic abyssal organic film, we find that approximately 10% of the gas-phase release reaches the sea surface. Integrated average injection depths for Arctic methane plumes will decrease by 50 - 300 m (for bubbles requiring oscillatory breakdown then shrinkage modulated by an organic surfactant coating). This effect significantly increases the likelihood of methane reaching the ocean-air interface. Giant boosts, large self-perpetuating bubbles, and coupling to the column and local saturation all leave open the possibility for much greater fractional transfer to the mixed layer. Uncertainties are mainly driven by the size distribution of the bubbles. Bubble dimensions at the source function will likely be determined to a large degree by fracturing, grain sizes, and channel networks in the seafloor, but these quantities are not yet well understood, and they have so far gone largely unsimulated.

In the original ocean circulation runs [Elliott et al., 2011], methane released at the sea floor but protected from oxidation due to oxygen and other resource limitations reached the atmosphere at a fractional efficiency of 10% or more (Section 3.1). This ratio will increase significantly as buoyant uplift is introduced. The possibility of bubble-plume transport of methane to the sea surface in the short term, plus a longer-term possibility of 10%-60% aqueous transport under resource limitation effects, calls into question the long-held assumption that only “about 1%” of any methane released into the ocean, at any level, can reach the atmosphere.

4. Atmospheric processes

Although this study has not involved in the development of new atmospheric models, the results of this project have led other groups, including scientists in the Climate department of the Earth Sciences Division at LBNL and colleagues at LLNL, to add additional methane-related capabilities to the atmospheric components of CESM. CESM1/CAM4 now includes fast methane chemistry in the general release version, Preliminary work by these groups has assessed climate sensitivity to methane emissions, establishing a background methane cycle, investigating the effects of methane from various sources (industry, farming, thawing permafrost, etc.).

These climate-atmosphere simulations suggest that an addition of 100 Tg/yr CH_4 roughly marks the boundary at which a methane source becomes significant in comparison to current global background emissions of 500 – 600 Tg/yr [Meehl et al., 2007]. By coincidence, the seafloor methane releases in Section 2 are estimated to be in the range of 80 – 140 Tg/yr (~10^{15} mol/yr), and with enhanced water column transport of methane via the processes discussed in Section 3, the possibility of a 20% or greater increase in methane emission due solely to dissociating hydrates is within the reasonable bounds of uncertainty.

Methane releases into the atmosphere, as with release into the water column, have consequences for atmospheric chemistry as well. Methane reaction pathways may lead to increases in tropospheric ozone, with localization due to circulation and the emission of other species, that may be significant as contributors to smog and lower air quality. The same methane releases can also result in increased stratospheric water vapor, increased polar stratospheric clouds, and as a result decreased *stratospheric* ozone in the polar regions [Cameron-Smith and Bhattacharya, personal communication]. It is also notable that atmospheric processes are almost entirely driven by the *rate* of methane release into the atmosphere, with total or cumulative release only significant in terms of the total carbon injected (i.e., the analysis of Archer [2007]). High rates in the short-term can drive short-term temperature changes, while slow ramping-up of methane releases would produce a much less dramatic feedback.

Conclusions, Current Work, and Future Directions

The Clathrate Gun Hypothesis focused on large-scale, rapid release of methane from seafloor hydrates in quantities large enough to 1) result in widespread injection of methane into the atmosphere, and 2) cause rapid warming feedbacks. Our research has strongly suggested that the release of methane from hydrates is actually likely to be:

1) Regional, rather than global
2) Persistent, rather than explosive
3) Limited by the magnitude of warming expected in the near term, from pre-industrial times through 2100
4) Mitigated by a number of factors in the sediments, including:
    a. Limits to the rate at which heat can be transported through sediments via conduction and advection
    b. The endothermic nature of hydrate dissociation
    c. Slow transport of methane in the sediments without overpressure driving flow, including the retention of a large fraction of the methane in the short term
5) Mitigated by factors in the water column, including:
    a. Oxidation by methanotrophs
    b. Transport into deep water (guaranteeing complete oxidation) through Arctic polar currents that feed the deeper ocean
    c. The limited set of circumstances under which bubble plumes or other fast transport pathways to the atmosphere can form.
6) Significant as an climate forcing only in cases of rapid release directly to the atmosphere

However, the research also indicates that:

1) Significant quantities of methane can still be released from hydrates as a result of predicted ocean warming scenarios
2) Methane will continued to be released over many centuries, even if warming stops
3) Long-term prospects are for continued and significant ocean warming, further extending the time of potential release
4) These quantities are likely to be globally significant, even if feedbacks are not triggered
5) The biochemical consequences of the released methane in the water column are an issue of real concern, and this issue has not been quantitatively addressed before
6) Resource limitations may hinder methane consumption, and the consumed resources may upset other aspects of ocean biology
7) Releases of methane into the atmosphere below the threshold for fast radiative feedbacks may still have chemical consequences in the troposphere and stratosphere.

As a net assessment, this analysis suggests a limited view of the direct climate impact of hydrates, at least as a fast positive feedback or "global disaster scenario." However, the research performed during this project has led to new insights about other aspects of hydrates and global climate. Even if rapid feedbacks do not occur, the biochemical and chemical consequences to the oceans and atmosphere demand further investigation, and in the long term, the vast quantities of carbon stored as shallow hydrates are likely to find their way into the oceans and atmosphere though some combination of the above-mentioned mechanisms. Therefore the reality is likely to be between the methane-driven climate shocks of Kennett and colleagues [2000] and the long-term view of hydrates as only another long-term contributor to total CO_2 in the atmosphere [Archer, 2007].

Even if not catastrophic in magnitude, the methane fluxes shown here are still within the range of potential climate sensitivity, such that recent developments in bubble-plume modeling and nutrient-limitation effects in the water-column biochemical filter will factor into fully understanding the range of climate impacts potentially driven by hydrates. In addition, understanding how climate-sensitive hydrates couple to other methane-transport problems—i.e., how the formation and dissociation of hydrates on the margin may regulate the transport of methane from other, deeper sources [Thatcher et al., 2013]—will be necessary, as this study focused only on hydrate-driven feedbacks by themselves.

At the time of this report, coupled climate/ocean models (which proceed on multi-month to multi-year schedules) continue to generate results. This report will be updated as new data arrives, although the key insights in Sections 1-4 will hold even if the range of possible outcomes is narrowed. Follow-on studies need to examine longer time horizons, as warming penetrates to deeper and deeper waters (as presumed) a thicker "bathtub ring" of sensitivity is likely to be affected. As the time window expands, the likelihood of large-scale hydrate dissociation increases, even if rates are constrained. Future work also needs to include field studies and direct observation of shallow hydrate systems, which may confirm the predicted scarcity of climate-driven methane release at the current time and also provide better data to constrain subseafloor, ocean, and atmospheric models used to predict future behavior.

Communications and Tech Transfer

This work overall has pioneered the quantitative assessment of the risks of hydrate-driven climate feedbacks, with six published papers (with 114 citations), 20 presentations (6 invited talks, 8 other talks, 6 posters), and 5 features in the popular scientific press.

Two papers are currently in preparation concerning the new results presented in this report:

Scott Elliott, "Systems Model Representation of Ocean Bubble Plumes Over Decomposing Arctic Clathrates"
Matthew Reagan, "Geological and Thermodynamic Constraints on the Release of Hydrate-Derived Methane in Response to Climate Change"

Recent conference presentations of this material have been limited, due to DOE travel restrictions for large conferences and events.

References

Archer D. (2007). Methane hydrate stability and anthropogenic climate change. *Biogeosciences* 4, 521-544.

Biastoch, A., Treude, T., Rupke, L.H., Riebesell, U., Roth, C., Burwicz, E.B., Park, W., Latif, M., Boning, C.W., Madec, G., Wallmann, K. (2011) Rising arctic ocean temperatures cause gas hydrate destabilization and ocean acidification. *Geophys. Res. Lett.* 38, L08602 http://dx.doi.org/10.1029/2011GL0472222.

Elliott, S.M., Reagan, M.T., Moridis, G.J., Cameron-Smith, P.J., (2010) "Geochemistry of Clathrate-Derived Methane in Arctic Ocean Waters," *Geophys. Res. Lett.*, 37, L12607, doi:10.1029/2010GL043369.

Elliott, S.M., Maltrud, M., Reagan, M.T., Moridis, G.J., Cameron-Smith, P.J. (2011), Marine Methane Cycle Simulations for the Period of Early Global Warming. *J. Geophysical Res. Biogeo. 116*, G01010.

Hedges, J., J. Baldock, Y. Gelinas, C. Lee, M. Peterson, S. Wakeham (2000) Evidence for non-selective preservation of organic matter in sinking marine particles. *Nature* 409, 801-804.

Hunter, S.J, Goldobin, D.S., Haywood, A.M., Ridgwell, A., Rees, J.G. (2013) Sensitivity of the global submarine hydrate inventory to scenarios of future climate change, *Earth & Planetary Sci. Lett.* 367, 105-115.

Kennett J.P., Cannariato K.G., Hendy L.L., Behl R.J. (2000) Carbon isotopic evidence for methane hydrate instability during quaternary interstadials. *Science* 288: 128-133.

Leifer, I., McDonald, I. (2003) Dynamics of the gas flux from shallow gas hydrate deposits: Interactions between hydrate bubbles and the oceanic environment. *Earth Planet. Sci. Lett*. 210, 411-424.

Leifer, I., Patro, R. (2002) The bubble mechanism for methane transport from the shallow sea bed to the surface: A review and sensitivity study. *Cont. Shelf. Res.* 22, 2409-2428.

Leifer, I., H. Jeuthe, S. Helge, V. Johansen (2009) Engineered and natural marine seep, bubble-driven buoyancy flows, *J. Phys. Oceanogr*. 39, 3071-3089.

Meehl G, Stocker T.F., Collins W.D., and 12 others. Global climate projections, In: *Climate Change 2007: The Physical Basis,* In IPCC AR4, Cambridge University Press, 2007.

Moridis, G.J., Kowalsky, M.B., Pruess, K. (2008) *TOUGH+HYDRATE v1.0 User's Manual: A Code for the Simulation of System Behavior in Hydrate-Bearing Geologic Media,* Report LBNL-0149E, Lawrence Berkeley National Laboratory, Berkeley, CA.

Reagan, M.T., Moridis, G.J., Elliott, S.M., Maltrud, M. (2011a), Contributions of Oceanic Gas Hydrate Dissociation to the Formation of Arctic Ocean Methane Plumes, *J. Geophys. Res. Oceans*, *116*, C09014, doi: 10.1029/2011JC007189.

Reagan, M.T., Moridis, G.J., Elliott, S.M., Maltrud, M., Cameron-Smith, P.J., (2011b). Basin-Scale Assessment of Gas Hydrate Dissociation in Response to Climate Change, *Proc*. 7th International Conference on Gas Hydrates, Edinburgh, Scotland, UK, 17-21 July 2011.

Reagan, M.T., Moridis, G.J. (2008), Dynamic response of oceanic hydrate deposits to ocean temperature change, *J. Geophys. Res*., *113*, C12023, doi:10.1029/2008JC004938.

Reagan, M.T, Moridis, G.J., Zhang, K., (2008) Modeling of Gas Hydrate Instability and Methane Release in Response to Climate Change, *Proc.* of the 6th International Conference on Gas Hydrates, Vancouver, BC, July 6-10, 2008.

Rehder. G., P. Brewer, E Peltzer, G. Friederich (2002) Enhanced lifetime of methane bubble streams within the deep ocean. *Geophys. Res. Lett*. 29, 10.1029/2001GL013966.

Thatcher, K. E., G. K. Westbrook, S. Sarkar, T. A. Minshull (2013), Methane release from warming-induced hydrate dissociation in the West Svalbard continental margin: Timing, rates, and geological controls, *J. Geophys. Res.*, *118*, doi:10.1029/2012JB009605.

van Vuuren et al. (2011). The Representative Concentration Pathways: An Overview. *Climatic Change*, 109 (1-2), 5-31.

Westbrook, G. and 19 others (2009) Escape of methane gas from the seabed along the West Spitsbergn continental margin. *Geophys. Res. Lett*. 36, 10.1029/2009/GL039191.